Ailanthone decreases cell viability in tongue squamous cell carcinoma via PI3K/AKT pathway

shuhan wang (1624280310@qq.com)
Binzhou Medical University - Yantai Campus https://orcid.org/0000-0001-8677-7192
Xiaoyu Chen
Binzhou Medical University - Yantai Campus
Xuejie Zhu
Binzhou Medical University - Yantai Campus
Kehao Lin
Binzhou Medical University - Yantai Campus
Qixiao Cui
Binzhou Medical University - Yantai Campus
Qiusheng Zheng
Binzhou Medical University - Yantai Campus
Defang Li
Binzhou Medical University - Yantai Campus https://orcid.org/0000-0003-4151-9151
Yuliang Wang
Binzhou Medical University - Yantai Campus

Research Article

Keywords: Ailanthone, tongue squamous cell carcinoma, apoptosis, PI3K/AKT pathway, cell cycle arrest

Posted Date: September 20th, 2021

DOI: https://doi.org/10.21203/rs.3.rs-911669/v1

Ailanthone decreases cell viability in tongue squamous cell carcinoma via PI3K/AKT pathway

Shuhan Wang[a,b†], Xiaoyu Chen[a†], Xuejie Zhu[a], Kehao Lin[b], Qixiao Cui[b], Qiusheng Zheng[a,c], Yuliang Wang[b,d*], and Defang Li[a*]

[a]School of Integrated Traditional Chinese and Western Medicine, Binzhou medical University, Yantai 264003, Shandong, China.

[b]College of Stomatology, Binzhou Medical University, Yantai 264003, Shandong, China.

[c]Key Laboratory of Xinjiang Endemic Phytomedicine Resources of Ministry of Education, School of Pharmacy, Shihezi University, Shihezi 832002, Xinjiang, China.

[d]Department of Oral and Maxillofacial Surgery, Yantai Affiliated Hospital of Binzhou Medical University, No 717, Jinbu Street, Muping District, Yantai, 264100.

* Correspondence:

Defang Li

lidefang@163.com, ORCID:0000-0003-4151-9151

Yuliang Wang

wangyuliang121@126.com

[†]These authors have contributed equally to this work and share first authorship.

Running title: Ailanthone decreases cell viability in tongue squamous cell carcinoma

ABSTRACT

To investigate the anti-tumor effect and mechanisms of ailanthone (AIL) in tongue squamous cell carcinoma (TSCC). The viability and apoptotic cell number of TCA8113 and Cal-27 cells declined and increased considerably following AIL. Hoechst 33258 staining revealed chromatin aggregation after exposure to AIL. Along with an accumulation of cleaved caspase-9, caspase-3, and PARP1, Bcl-2/Bax ratio and the levels of caspase-3, caspase-9 and PARP1 reduced after exposure to AIL treatment. Subjecting Cal-27 cells to AIL treatment led to the arrestment of the cell cycle at the G2/M phase. Nevertheless, the cell cycle of AIL-treated TCA8113 cells did not change significantly. Following AIL treatment, a decline in the expression of CDK1 and cyclin B1 was manifested by Western Blot. The p-AKT as well as the expression level of p-PI3K underwent a significant downregulation by AIL in both cells. The outcome furnishes a valuable understanding of the potential applications of AIL in treating TSCC.

KEYWORDS: Ailanthone, tongue squamous cell carcinoma, apoptosis, PI3K/AKT pathway, cell cycle arrest

1. Introduction

As a common and highly malignant oral squamous cell carcinoma, tongue squamous cell carcinoma (TSCC) [1] TSCC can easily lead to disorders of swallowing, chewing, speech thereby seriously influencing the quality of life of the patient [2]. It also has a poor prognosis and a high local recurrence rate, which lead to reduced overall survival rate. In recent years, death rate caused by TSCC has increased significantly, and the incidence of TSCC has shifted to a younger age [3]. The major therapeutic strategy for TSCC involves multidisciplinary collaborative comprehensive sequential therapy comprising surgical intervention. Unfortunately, eating, breathing, speech and other functional dibilities are a frequent unfavorable outcome of the surgical treatment. The extreme cases may involve a maxillofacial deformity TTSC has a significantly large rate of recurrence rate and a propensity to metastasize to remote organs as well as lymphnote [4]. Find new treatment methods for TSCC is thus a major concern for the scientific community.

Traditional Chinese medicines (TCM) have recently been gaining quite a lot of attention, particularly in terms of their antitumor influence, pharmacological characteristics, and relatively few side effects. The therapeutic role of TCM is exerted upon the body in a sophisticated manner via restoration of normal balance. Additionally, the specialists of traditional Chinese medicine tend to enhance and strengthen the inherent body resistance against diseases and work towards customization of therapy for individuals. Naturopathic therapy with TCM is chosen by a high number of patients, considering that these substances are considered as multicomponent, multitarget, and multistage agents. TCM approach is being accepted by more and more people all over the world.

Ailanthone (AIL), a chemical substance from nature, obtained from the bark and whole seedlings of traditional Chinese medicine Ailanthus altissima (Mill.) Swingle, has a wide range of biological activities [5]. Traditionally, Ailanthus altissima (Mill.) Swingle was utilized for treating ascariasis, spermatorrea, gastrointestinal diseases, diarrhea, bleeding, and inflammation [6, 7]. In several cancer cell lines, AIL was observed to exert growth inhibitory effects in vitro and in vivo [8]. Ni et al. found that in non-small cell lung cancer (NSCLC), the cell growth and colony generation were suppressed by AIL in vitro. It also blocked NSCLC growth of tumor in subcutaneously xenografted and orthotopic lung tumor prototypes,

thereby prolonging the survival span of tumor-bearing mice [9]. AIL instigated the arrest of the G0/G1-phase of the cell cycle, as implied by the decline in the expression of CDKs and cyclins and an elevated expression of p27 and p21 in hepatocellular carcinoma (HCC) [10]. MDA-MB-231 cells also manifested an inhibition in their proliferation, migration, and invasion by regulating miR-148a upon exposure to AIL [11].

To date, there have been no studies about the influence and mechanism of action of AIL on human TSCC. Therefore, this work was taken up for addressing the influence of AIL on TSCC in vitro and clarify its potential mechanism.

2. Materials and methods

Chemicals and Reagents

The acquisition of Ailanthone (AIL) (purity ≥ 98%) was from Jiangxi Herb Tiangong Technology (Jiangxi, China). The acquisition of Dulbecco's Modified Eagle's Medium (DMEM) and RPMI-1640 medium was from HyClone laboratories, Inc. (Logan, UT). In addition, 3-(4,5-dimethylthiazol-2-yl)-2,5-diphenyltetrazolium-bromide (MTT), phenylmethylsulfonyl fluoride (PMSF), and RIPA lysis buffer were provided by Sigma-Aldrich (Steinheim, Germany). Fetal bovine serum (FBS) was acquired from Thermo Fisher Scientific, Co Ltd, China. The possession of Penicillin/streptomycin (1:100), Hoechst 33258 dye, protease and phosphatase inhibitors, cell-cycle detection kit (CCDK), Annexin V-FITC Apoptosis Detection Kit (ADK) along with propidium iodide (PI) were acquired from a China company (*i.e.,* Solarbio, Inc, Beijing). BCA-protein assay kits were provided by Nanjing KeyGen Biotech Co., Ltd. (China). Cleared-PARP1 (ab32064, 1:5000), PARP1 (ab191217, 1:1000), cleared caspase-3 (ab32042, 1:500), and cleared caspase-9 (ab2324, 1:1000) antibodies were purchased from Abcam. Bax (cat. no. 5023S, 1:1000), Bcl-2 (cat. no. 4223S, 1: 1000), caspase-3 (cat. no. 14220S, 1:1000), caspase-9 (cat. no. 9502S, 1:1000), p-PI3K (cat. no. 17366, 1:1000), PI3K (cat. no. 60225-1, 1:1000), p-AKT (cat. no. 4060, 1:1000), AKT (cat. no. 9272, 1:1000), and β-actin (cat. no. 4970S, 1:1000) antibodies were purchased from CST Biological Reagents Co., Ltd. (Shanghai, China), while horseradish peroxidase-conjugated antirabbit Immunoglobulin G (cat. no. D110065) was purchased from

Sangon Biotech Co., Ltd (Shanghai, China). Other common chemicals were provided by company, Shanghai Titanchem Co., Ltd. China.

Cell Culture

The acquisition of Human tongue squamous cell carcinoma Cal-27 and TCA8113 cells were from Yantai Bayu Biotechnology Co. Ltd. Both types of cells (Cal-27 and TCA8113) were seeded in DMEM (89%) comprised of 1% antibiotic (*i.e.,* streptomycin or penicillin) and FBS (10%). The cells were cultured in a sterile incubator (HF240, HEALFORCE, Shanghai Lishen Scientific Equipment Co. Ltd.). After the cells had grown to about 80% of the culture flask, passaging was carried out, and the passage was carried out once in a ratio of 3:1 in about 2–3 days.

MTT Assay

In each well of 96-well plates, 5×10^3 Cal-27 and TCA8113 cells in the logarithmic growth phase were cultured separately. The culture mixture of both types of cells was incubated overnight with 5% continuous supply of CO_2 at 37 ˚C. The grown cells were exposed to various concentrations of AIL (0, 0.25, 0.5, 1, 2, 4, 8, 16, and 32 μM). After 24 hrs of incubation, the underlined cells were treated with 5 mg/mL of MTT solution (prepared in PBS) for 4 hrs. The absorbance of the converted dye was recorded at 595 nm via microplate reader (Infinite M200 PRO, Tecan Group, Ltd., Mannedorf). The obtained data was compared with the control.

Hoechst 33258 Staining

Hoechst 33258 staining was carried out to evaluate morphological variations in cell nuclei, as shown earlier (Amirbekyan et al., 2020). The seeding of Cal-27 and TCA8113 cells (5×10^4 cells/mL in each well) was carried out in 24-well plates, followed by overnight incubation. The cells incubation was carried out

with different concentrations (0.25, 1, and 4 μM) of AIL for 24 hrs. After the incubation, PBS was utilized for cells washing while paraformaldehyde (4%) was used for cells fixation at ~ 25°C for 10 min. Then cleaned again with PBS, the cells were cleaned with Hoechst 33258 staining solution in the dark for 10 min. Finally, the cells washing was carried out twice with PBS, the images of the stained nuclei were captured by a fluorescence microscope (DMI3000B, Leica, Leica Microsystems CMS GmbH).

Evaluation of Apoptosis by Flow Cytometry

Apoptosis was investigated via Annexin V-FITC /PI ADK. Next, the seeding of 2×10^5 Cal-27 and TCA8113 cells was conducted in the logarithmic growth phase onto 6-well plates at 37˚C and CO_2 (5%) for 24 hrs. Post 24 hrs of application of AIL (0.25, 1, and 4 μM), the cells washing was carried out twice with PBS, followed by resuspending in Annexin V binding buffer (400 μL). Furthermore, the cells incubation was carried out with Annexin V（5 μL, conjugated with FITC）and PI (5 μL) for 15 min in the dark at ~ 25°C. FACScan flow cytometer and BD FACSuite™ software were used to analyze the apoptotic cells.

Analysis of Cell Cycle

Logarithmic growth phase of cells (2×10^5) *i.e.,* Cal-27 and TCA8113 cells were inoculated on 6-well plates. The second day, when the cell density reached about 70%, different concentrations of AIL were added, followed by overnight incubation. The 6-well plates were taken out and the cells were collected. The precooled 75% alcohol was separately added and placed at 4°C for 24 hrs. On the next day, the cells were cleaned with cold PBS, and then centrifuged, followed by addition of 100 μL RNase A (Cat. No. CA1050, Solarbio, China), incubation in water bath at 37°C for 30 min, and addition of 400 μL PI staining solution. Next, the cells incubation was carried out in dark for 0.5 hrs (at 4°C). Finally, the cell cycle phases were evaluated via flow cytometry.

Western Blotting

Logarithmic growth phase of 2×10^6 cells *i.e.,* Cal-27 and TCA8113 were inoculated on Petri dishes (100-mm). Next, either vehicle or AIL treated the cells. After that, the cells washing (twice) were carried out with cold PBS, followed by solubilizing in lysis buffer with phosphatase and protease inhibitors. The BCA protein detection kit were used for Protein concentration. The protein separation using a total of 40 μg cell lysate were used by 10% SDS-PAGE, followed by protein transferring to PVDF membranes (EMD Millipore). In 2 hours,PVDF membranes were blocked with 5% nonfat milk under the condition of room temperature. Then, the PVDF membrane diluted in 5% nonfat milk in TBST with Tween 20 (0.1%) was incubated with special antibodies or anti-β-actin as housekeeping protein. Subsequently,horseradish peroxidase-conjugated IgG served as secondary antibody were used for the incubation.The detection of secondary antibodies on the PVDF membrane were used by the enhanced chemiluminescnce (ECL) detection reagents (Pierce; Thermo Fisher Scientific, Inc.). densitometry analysis (including integrated density of bands) was carried out via Image J (NIH), followed by normalizing the documented values to beta-actin.

Statistical Analysis

All experimental procedures were evaluated thrice. The obtained results were indicated as mean ± SD. Statistical analysis have applied for SPSS (ver 20.0 Chicago, IL) and use GraphPad Prism 6.0 software to visually indicate the variations between the control and the experimental group. One-way ANOVA was used to determine the variations between groups. $P < 0.05$ was regarded as statistically considerable.

3. Results

AIL inhibits the proliferation and induces apoptosis of TSCC cells

A range of concentrations (0, 0.25, 0.5, 1, 2, 4, 8, 16, and 32 μm) of AIL was employed in an MTT assay to detect the cell activity for 24 h. (Figure 1A and Figure 1B) showed that that the viability of Cal-27

and TCA8113 cells reduced significantly (The IC_{50} values corresponding to Cal-27 cells and TCA8113 cells were 0.8807 and 0.7884, respectively. With different concentrations of AIL, the total count of TCA8113 and Cal-27 cells decreased under an inverted fluorescence microscope. Hoechst 33258 staining revealed that the shape of nuclei shrank in TCA8113 and Cal-27 cells after the exposure to AIL. Following 1 μM and 4 μM AIL treatment, the signal of chromatin aggregation was observed in TCA8113 cells and Cal-27 (Figure 1C and Figure 1D). Flow cytometry was further used to detect apoptosis by using double staining based on Annexin V-FITC/PI. When juxtaposed against the control group, amongst the TCA8113 and Cal-27 cells, the number of cells in the early and late stages of apoptosis manifested a dose-dependent increase (Figure 1E and Figure 1G). As shown in Figure 1F and Figure 1H, apoptotic cells had a percent count of 17% in TCA8113 cells and 39% in Cal-27.

AIL induces mitochondrial-mediated apoptosis in TSCC cells

Previous results showed that AIL treatment of TCA8113 and Cal-27 cells subsequently resulted in an increment in the count of apoptotic cells in the early and late stages. To further confirm that AIL induces Cal-27 and TCA8113 cell apoptosis, we employed western blot for detecting the expression of proteins associated with apoptosis. We found that Bcl-2/Bax ratio decreased significantly after 1 μM AIL and 4 μM AIL in both TCA8113 and Cal-27 cells in comparison with the control group (Figure 2A–B and Figure 2E–F). The determination index was the ratio of target gene gray values and housekeeping gene gray values. We found that following AIL exposures, the expression of caspase-9, caspase-3, and PARP1 underwent a decrease, simultaneously accompanied by cleaved caspase-9, caspase-3, and PARP1 accumulating in significant quantities within TCA8113 and Cal-27 cells. The outcome in our work implies that the inherent apoptotic pathway was primarily responsible for apoptosis induced by AIL in TCA8113 and Cal-27 cells.

AIL triggers the arrest of the cell cycle in Cal-27 cells in the G2/M phase but does not influence TCA8113 cells

188 To ascertain if the cell cycle progression is affected by AIL, we subjected Cal-27 and TCA8113 cells to
189 treatment with a range of concentrations of AIL for a duration of 24 h, followed by flow cytometric
190 analysis of the cell cycle distribution. It was evident that only Cal-27 cells treated with 4 μL AIL
191 manifested a considerable reduction in the ratio of cells within the G0/G1 state in comparison to the control
192 cells (Figure 3A and Figure 3B). The total count of Cal-27 cells observed in the G2/M phase exhibited a
193 significant increment upon treating with 1 μM and 4 μM AIL compared with control (Figure 3A and Figure
194 3B). The cell number in S phase increased significantly after treatment with 4 μM AIL (Figure 3A and
195 Figure 3B). Thereafter, we made a thorough assessment of the molecular mechanism regulating cell cycle
196 arrest in Cal-27 cells induced by AIL. Western blotting was employed to estimate the G2/M-related proteins.
197 As evident from Figure 2C and 2D, AIL decreased the expression level of CDK1 and cyclin B1, which
198 implied that AIL induced the arrest of G2/M in Cal-27 cells. We also analyzed the cell cycle change in
199 TCA8113 cells. The fraction of cells in various cell cycle phases did not differ among the AIL treatments in
200 TCA8113 cells. Therefore, we did not further detect the transition in the expression of proteins taking part
201 in the cell cycle (Figure 3E and Figure 3F).

202

203 *AIL causes blocking of the PI3K/AKT pathway in TSCC cells*

204 To probe into the molecular level mechanistic pathway controlling apoptosis and G2/M phase arrest
205 mediated by AIL, an analysis of the expression of proteins associated with the PI3K/AKT pathway was
206 carried out. As illustrated in Figure 4A and Figure 4B, the expression level of phospho-PI3K p55 subunit
207 was significantly downregulated by AIL in Cal-27 cells. As evident in Figure 4B, the extent of expression
208 of PI3K was not found to alter significantly in Cal-27 cells. From Figure 4A and Figure 4B, it can be seen
209 that the phosphorylation of AKT at the Ser473 site also decreased after AIL treatment in Cal-27 cells. In
210 Cal-27 cells, only after the treatment with 4 μM AIL, the expression of total AKT increased significantly
211 (Figure 4B). In TCA8113 cells, there was a significant down-regulation in the expression level of
212 phospho-PI3K p55 subunit and phosphorylation of AKT at the Ser473 site by AIL (Figure 4C and Figure
213 4D). The expression level of PI3K increased significantly after 0.25, 1, and 4 μM AIL in TCA8113 cells
214 (Figure 4D), while the expression level of total AKT decreased significantly after the treatment with 0.25, 1,

215 and 4 μM AIL (Figure 4D).

216

217

218 **4. Discussion**

219 Tongue squamous cell carcinoma (TSCC) is an aggressive form of cancer of the oral cavity which
220 invades rapidly and has the highest rate of prevalence and recurrence among the various kinds of oral
221 cancers [1]. In 2015, within China, a total of 48,100 new cases and 22,100 deaths associated with TSCC
222 were reported [12]. Although the clinical outcomes have been improved after the advances in radiotherapy,
223 chemotherapy, and surgical therapy, the prognosis, in general, and the overall survival rates of TSCC
224 patients have not improved much over the last decade. Hence, it is necessary to explore and find improved
225 drugs for developing novel therapeutic approaches for TSCC patients.

226 TCM has an extensive background of successful utilization in the treatment as well as prevention of
227 disorders and diseases. Research studies and clinical observations have revealed that traditional herbal
228 Chinese medicines as well as their extracts have powerful inhibitory characteristics against tumors [13, 14].
229 AIL, a compound acquired from the Chinese traditional medicine Ailanthus altissima, has anticancer
230 potential toward a multitude of cancer cell lines. According to the findings of the present work, the viability
231 of TCA8113 and Cal-27 cells decreased significantly following AIL treatment. Exposure to AIL led to
232 chromatin aggregation as revealed by Hoechst 33258 staining. After the treatment with AIL, the count of
233 apoptotic cells in the early and late stages of apoptosis among Cal-27 and TCA8113 types increased in
234 comparison with the control group. Bcl-2/Bax ratio and the levels of caspase-9, caspase-3, and PARP1
235 underwent a decline following treatment with AIL, while Cal-27 and TCA8113 cells manifested an
236 accumulation of cleaved caspase-9, cleaved caspase-3, and cleaved PARP1. Cal-27 cells, following AIL
237 treatment, proceeded to seize the cell cycle at the G2/M phase. The expression of CDK1 and cyclin B1
238 decreased after the AIL exposure. In contrast, the cell cycle of TCA8113 cells did not alter significantly
239 following the AIL treatment. It has also been reported by previous works that the same drug could lead to
240 arresting the cell cycle, however, various cells were seized at varying phases of the cellular cycle. Lou et al.

241 treated A549 cells and human B lymphoblastoid cells with different concentrations of hexavalent chromium
242 [Cr(IV)] (0, 5 mM, 10 mM, and 15 mM) for 2 h and 24 h. The relative ratio of cells in G0/G1 and S phases
243 of human B lymphoblastoid cells changed significantly, while G0/G1 and G2/M phases changed
244 significantly in A549 cells. The authors speculate that different drug effects may be related to different
245 cellular metabolic patterns [15]. In addition, we observed that the expression level of phospho-PI3K p55
246 subunit and the phosphorylation of AKT at the Ser473 site were significantly downregulated by AIL both in
247 TCA8113 cells and Cal-27 cells.

248 At the molecular level, we found that the expression of Bcl-2 and CDK1 decreased significantly after
249 the AIL treatment. It has been reported that Bcl-2 mainly has an antiapoptotic function, but multisite
250 phosphorylation can cause it to lose this function [16]. According to Zhou et al., a candidate Bcl-2 kinase,
251 CDK1, has been reported to phosphorylate Bcl-2 [17]. That means that Bcl-2 expression is closely related
252 to apoptosis and cell cycle. Decreased concentrations of Bcl-2 can stimulate the death of cells and can
253 additionally regulate the cell cycle [18]. Bcl-2 overexpression caused a substantial delay in the S phase
254 entry of quiescent NIH 3T3 fibroblasts induced by serum stimulation [19]. The involvement of CDK1 in
255 the cell cycle progression to the M phase from the G2 phase is quite well known [20]. Some studies
256 reported a proapoptotic activity of CDK. Cyclin B1/CDK1 upon upregulation regulates apoptosis following
257 2-methoxyestradiol-induced mitotic catastrophe [21]. Zhang et al. documented that CDK1 protein has an
258 involvement in the apoptosis and proliferation of cells in ovarian cancer [22]. According to Chu et al., in
259 KB-3 cells, CDK1/cyclin B has an indispensable role in apoptosis induced by the mitotic arrest that takes
260 place by phosphorylation of Mcl-1 [23]. Based on the earlier studies, we speculate that the downregulation
261 of CDK1 expression induced by AIL prevents the Bcl-2 phosphorylation, which enables Bcl-2 to function
262 normally. However, the expression of Bcl-2 was downregulated by AIL, which prevented the antiapoptotic
263 effect of Bcl-2 and led to apoptosis of human tongue squamous cell carcinoma cells. We also discovered
264 that the cell cycle was seized in the G0 phase following treatment with 4 μM AIL. However, the more
265 obvious change was the effect of AIL on the cell cycle, the G2/M stage in particular. In general, the
266 reduction in Bcl-2 and CDK1 induced by AIL mediated the arrest of the cell cycle and regulation of
267 apoptosis in tongue squamous cell carcinoma.

In human cancers, the phosphoinositide 3-kinase (PI3K)-AKT pathway is the most recurrently triggered pathway regulating survival, differentiation, cell growth, cell metabolism, and cytoskeletal rearrangement of cells in response to a wide array of signals. It has been reported that phosphorylated AKT promotes the cell cycle-related protein cyclin D and apoptosis-related protein Bcl-2 [24]. The decline in the expression of AKT induces cell apoptosis while inhibiting Bcl-2 expression [25]. It was reported by Zhang et al. that in colorectal cancer, the inhibited phosphorylation of PI3K and AKT reduced Bcl-2 expression subsequently promoting the mitochondrial apoptosis induced by oxaliplatin [26]. According to several reports, the action of the PI3K/AKT signaling pathway can be promoted by CDK1 [27]. Specifically, Wu et al. found a decrease in CDK1 expression by shRNAs, accompanied by a significant downregulation in AKT [28]. The reports by Wang et al. suggested that CDK1 has the potential to further switch on PI3K/AKT pathway by targeting PDK1 phosphorylation. In this work, we confirmed the changed degree of expression of phosphorylated AKT and decreased expression of Bcl-2 in TSCC cells pre-treated with AIL. Therefore, we can speculate that the downregulation of CDK1 induced by AIL may affect the PI3K/AKT signaling pathway. The decreased CDK1 expression was accompanied by downregulation of AKT, which further brought about the decline in the expression of Bcl-2, eventually leading to TSCC apoptosis.

To the best of our awareness, the current work is a pioneer report demonstrating the antitumor effect of AIL on tongue squamous cell carcinoma. For a better understanding of the therapeutic capability of AIL, additional in vivo experiments are needed to verify the antitumor ability of AIL. Our observations conclusively demonstrated that AIL instigated the arrest of the cell cycle at G2/M and suppressed the PI3K/AKT signaling pathway to cause apoptosis of tongue squamous cell carcinoma cells. We, therefore, suggest that AIL shows prospects of being developed into an effective novel therapeutic agent focusing to target the PI3K/AKT pathway in tongue squamous cell carcinoma.

Disclosure statement

No conflicts of interest to declare.

Data availability statement

All datasets generated for this study are included in the article.

Author contributions

Conceptualization, X.C., D.L. and Y.W.. Methodology, S.W., X.C., X.Z., K.L. and Q.C.. Statistical analysis, X.C. and Q.Z.. Supervision, D.L. and Y.W.. Writing - original draft, X.C.. Writing - review & editing, D.L.. Funding acquisition, X.C., Q.Z. and D.L..

Funding

This work was supported by the National Natural Science Foundation of China (Grant No. 31471338 to Qiusheng Zheng), Scientific Research Foundation of Binzhou Medical University (Grant No. BY2014KYQD01 to Qiusheng Zheng and Grant No. BY2018KYQD07 to Xiaoyu Chen), Natural Science Foundation of Shandong Province (Grant No. ZR2020QH326 to Xiaoyu Chen), and the Dominant Disciplines' Talent Team Development Scheme of Higher Education of Shandong Province (to Defang Li).

References

References:

1. Gan R H, Lin L S, Zheng D P, et al. High expression of Notch2 drives tongue squamous cell carcinoma carcinogenesis. Exp Cell Res. 2021; 399(1): 112452.

2. Calabrese L, Pietrobon G, Fazio E, et al. Anatomically-based transoral surgical approach to early-stage oral tongue squamous cell carcinoma. Head Neck. 2020; 42(5): 1105-1109.

3. Majchrzak E, Szybiak B, Wegner A, et al. Oral cavity and oropharyngeal squamous cell carcinoma in young adults: a review of the literature. Radiol Oncol. 2014; 48(1): 1-10.

4. Zhu L, Wang Y, Li R, et al. Surgical treatment of early tongue squamous cell carcinoma and patient survival. Oncol Lett. 2019; 17(6): 5681-5685.

5. Ding H, Yu X, Hang C, et al. Ailanthone: A novel potential drug for treating human cancer. Oncol Lett. 2020; 20(2): 1489-1503.

6. Hou S, Cheng Z, Wang W, et al. Ailanthone exerts an antitumor function on the development of human lung cancer by upregulating microRNA-195. J Cell Biochem. 2019; 120(6): 10444-10451.

7. Cucci M A, Grattarola M, Dianzani C, et al. Ailanthone increases oxidative stress in CDDP-resistant ovarian and bladder cancer cells by inhibiting of Nrf2 and YAP expression through a post-translational mechanism. Free Radic Biol Med. 2020; 150: 125-135.

8. Peng S, Yi Z, Liu M. Ailanthone: a new potential drug for castration-resistant prostate cancer. Chin J Cancer. 2017; 36(1): 25.

9. Ni Z, Yao C, Zhu X, et al. Ailanthone inhibits non-small cell lung cancer cell growth through repressing DNA replication via downregulating RPA1. Br J Cancer. 2017; 117(11): 1621-1630.

10. Zhuo Z, Hu J, Yang X, et al. Ailanthone Inhibits Huh7 Cancer Cell Growth via Cell Cycle Arrest and Apoptosis In Vitro and In Vivo. Sci Rep. 2015; 5: 16185.

11. Gao W, Ge S, Sun J. Ailanthone exerts anticancer effect by up-regulating miR-148a expression in MDA-MB-231 breast cancer cells and inhibiting proliferation, migration and invasion. Biomed Pharmacother. 2019; 109: 1062-1069.

12. Chen W, Zheng R, Baade P D, et al. Cancer statistics in China, 2015. CA Cancer J Clin. 2016; 66(2): 115-32.

13. Tang K Y, Du SL, Wang Q L, et al. Traditional Chinese medicine targeting cancer stem cells as an alternative treatment for hepatocellular carcinoma. J Integr Med. 2020; 18(3): 196-202.

14. Gao Y, Chen S, Sun J, et al. Traditional Chinese medicine may be further explored as candidate drugs for pancreatic cancer: A review. Phytother Res. 2021; 35(2): 603-628.

15. Lou J, Wang Y, Yao C, et al. Role of DNA methylation in cell cycle arrest induced by Cr (VI) in two cell lines. Plos One. 2013; 8(8): e71031.

16. Zhou M, Zhang Q, Zhao J, et al. Phosphorylation of Bcl-2 plays an important role in glycochenodeoxycholate-induced survival and chemoresistance in HCC. Oncol Rep. 2017; 38(3): 1742-1750.

17. Zhou L, Cai X, Han X, et al. CDK1 switches mitotic arrest to apoptosis by phosphorylating Bcl-2/Bax family

proteins during treatment with microtubule interfering agents. Cell Biol Int. 2014; 38(6): 737-46.

18. Du X, Fu X, Yao K, et al. Bcl-2 delays cell cycle through mitochondrial ATP and ROS. Cell Cycle. 2017; 16(7): 707-713.

19. O'Reilly L A, Huang D C, Strasser A. The cell death inhibitor Bcl-2 and its homologues influence control of cell cycle entry. Embo J. 1996; 15(24): 6979-90.

20. Lim G, Chang Y, Huh W K. Phosphoregulation of Rad51/Rad52 by CDK1 functions as a molecular switch for cell cycle-specific activation of homologous recombination. Sci Adv. 2020; 6(6): eaay2669.

21. Choi H J, Zhu B T. Upregulated cyclin B1/CDK1 mediates apoptosis following 2-methoxyestradiol-induced mitotic catastrophe: Role of Bcl-XL phosphorylation. Steroids. 2019; 150: 108381.

22. Zhang R, Shi H, Ren F, et al. The aberrant upstream pathway regulations of CDK1 protein were implicated in the proliferation and apoptosis of ovarian cancer cells. J Ovarian Res. 2017; 10(1): 60.

23. Chu R, Terrano D T, Chambers T C. Cdk1/cyclin B plays a key role in mitotic arrest-induced apoptosis by phosphorylation of Mcl-1, promoting its degradation and freeing Bak from sequestration. Biochem Pharmacol. 2012; 83(2): 199-206.

24. Liu Z, Zhao L, Song Y. Eya2 Is Overexpressed in Human Prostate Cancer and Regulates Docetaxel Sensitivity and Mitochondrial Membrane Potential through AKT/Bcl-2 Signaling. Biomed Res Int. 2019; 2019: 3808432.

25. Dai Y, Jin S, Li X, et al. Correction: The involvement of Bcl-2 family proteins in AKT-regulated cell survival in cisplatin resistant epithelial ovarian cancer. Oncotarget. 2020; 11(4): 488-489.

26. Zhang L, Chen H, Song Y, et al. MiR-325 Promotes Oxaliplatin-Induced Cytotoxicity Against Colorectal Cancer Through the HSPA12B/PI3K/AKT/Bcl-2 Pathway. Dig Dis Sci. 2020.

27. Wang Y, Du X, Wang J. Transfer of miR-15a-5p by placental exosomes promotes pre-eclampsia progression by regulating PI3K/AKT signaling pathway via CDK1. Mol Immunol. 2020; 128: 277-286.

28. Wu C X, Wang X Q, Chok S H, et al. Blocking CDK1/PDK1/beta-Catenin signaling by CDK1 inhibitor RO3306 increased the efficacy of sorafenib treatment by targeting cancer stem cells in a preclinical model of hepatocellular carcinoma. Theranostics. 2018; 8(14): 3737-3750.

Figure legends

Figure 1. The proliferation of TSCC cells was inhibited by AIL and apoptosis was induced. (A) Chemical

structure of ailanthone. Seeding of (B) Cal-27 or (C) TCA8113 cells was done onto a 96-well plate followed by treatment with different concentrations (0.25, 0.5, 1, 2, 4, 8, 16, and 32 μM) of AIL for 24 h. *** $p < 0.001$, compared with the control. Influence of AIL on apoptosis among (D) Cal-27 or (E) TCA8113 cells, as detected by Hoechst 33258 staining. The apoptotic rate of (F) Cal-27 or (G) TCA8113 cells after AIL treatment for 24 h was detected by employing Annexin V-FITC/PI double staining. The percent count of apoptotic cells in Cal-27 or TCA8113 cells is shown in (H) and (I). ** $p < 0.01$, *** $p < 0.001$, in comparison with the control cells.

Figure 2. AIL induced apoptosis in TSCC by influencing Bcl-2/Bax ratio and caspase expression. (A) The protein expression of Bax and Bcl-2 in Cal-27 cells subjected to AIL treatment or otherwise were assessed by western blotting. (B) Statistical study of the Bcl-2/Bax ratio in Cal-27 cells with or without AIL. *** $p < 0.001$, compared with the control. (C) The degree of expression of cleaved PARP1, PARP1, cleaved caspase-9, caspase-9, cleaved caspase-3, and caspase-3 in Cal-27 cells was assessed by western blotting. (D) Statistical analysis of the expression of cleaved PARP1, PARP1, cleaved caspase-9, caspase-9, cleaved caspase-3, and caspase-3 in AIL-treated Cal-27 cells. * $p < 0.05$, ** $p < 0.01$, *** $p < 0.001$, in comparison with the control. (E) The protein expression of Bcl-2 and Bax in TCA8113 cells treated with or without AIL were examined by western blotting. (F) Statistical analysis of the Bcl-2/Bax ratio in TCA8113 cells with or without AIL. ** $p < 0.01$, compared with the control. (F) The extent of expression of cleaved PARP1, PARP1, cleaved caspase-9, caspase-9, cleaved caspase-3, and caspase-3 in TCA8113 cells were assessed by western blotting. (G) Statistical study of the expression of cleaved PARP1, PARP1, cleaved caspase-9, caspase-9, cleaved caspase-3, and caspase-3 in AIL-treated TCA8113 cells. * $p < 0.05$, ** $p < 0.01$, *** $p < 0.001$, in comparison with the control.

Figure 3. AIL induced cycle arrest in G2/M phase in Cal-27 cells, however did not have any influence on TCA8113 cells. (A) Flow cytometry was employed to analyze the cell cycle distribution changes in Cal-27 cells subjected to AIL treatment or otherwise. (B) Statistical analysis of the distribution of cell cycle in

Cal-27 cells treated with or without AIL. * $p < 0.05$, *** $p < 0.001$, compared with the control. (C) The expression levels of CDK1 and Cyclin B1 in Cal-27 cells treated with or without AIL, as assessed by western blotting. (D) Statistical study of the expression levels of CDK1 and Cyclin B1 in AIL-treated Cal-27 cells. ** $p < 0.01$, *** $p < 0.001$, in comparison with the control. (E) The changes in cell cycle distribution in TCA8113 cells subjected to AIL treatment or otherwise were measured by flow cytometry. (F) Statistical study of the cell cycle distribution in TCA8113 cells treated with or without AIL. However, no significant changes were apparent in the AIL-treated TCA8113 cells in comparison with the controls.

Figure 4. AIL decreased the proliferation of TSCC cells via the PI3K/AKT Pathway. (A) The extent of expression of p-PI3K, PI3K, p-AKT, and AKT in Cal-27 cells treated with or without AIL were ascertained by western blotting. (B) Statistical study of the expression levels of p-PI3K, PI3K, p-AKT, and AKT in the AIL-treated Cal-27 cells. * $p < 0.05$, ** $p < 0.01$, *** $p < 0.001$, in comparison with the control. (C) The expression levels of p-PI3K, PI3K, p-AKT, and AKT in TCA8113 cells treated with or without AIL were assessed by western blotting. (D) Statistical study of the expression levels of p-PI3K, PI3K, p-AKT, and AKT in the AIL-treated TCA8113 cells. * $p < 0.05$, ** $p < 0.01$, *** $p < 0.001$, in comparison with the control.

Figures

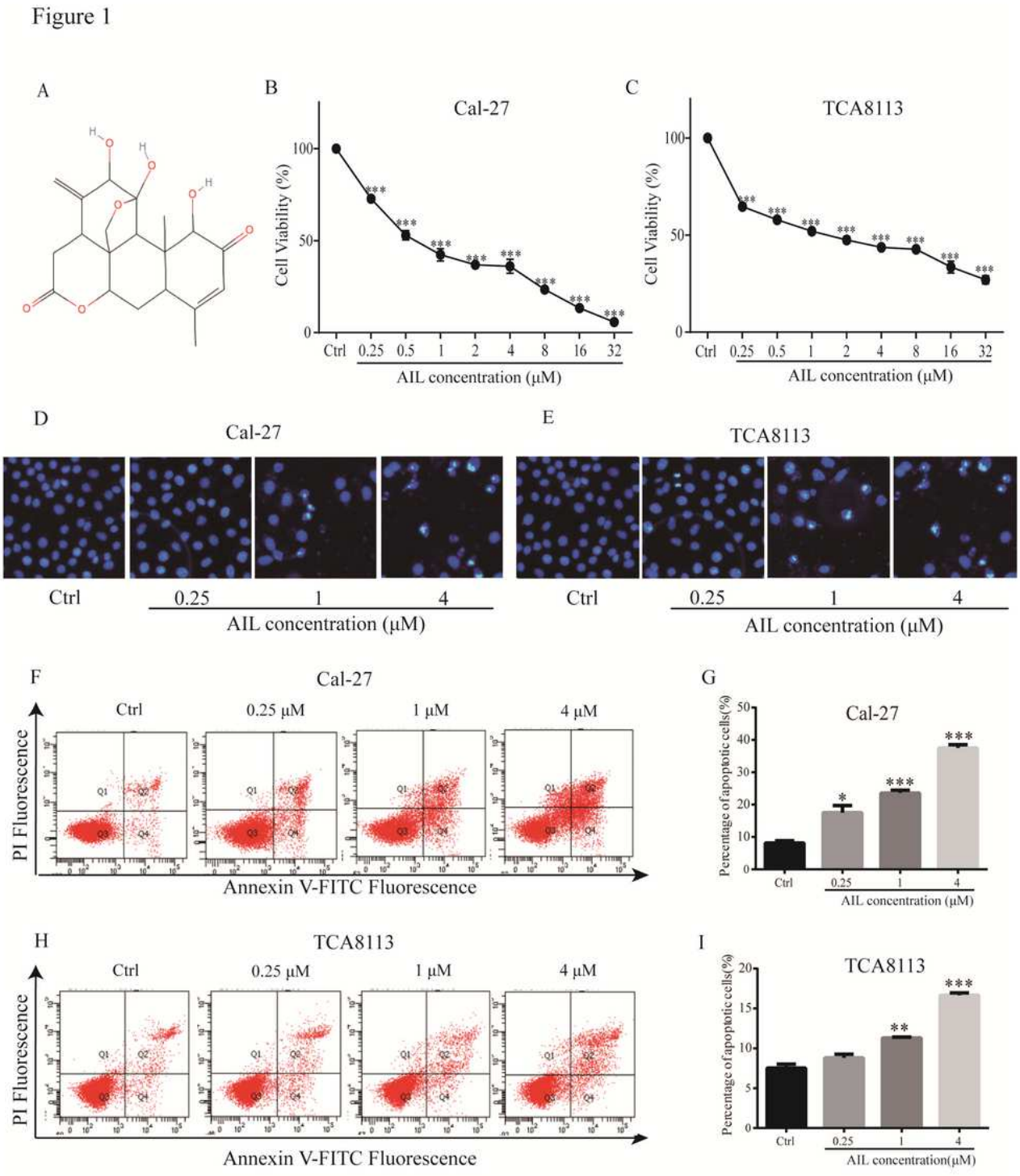

Figure 1

The proliferation of TSCC cells was inhibited by AIL and apoptosis was induced. (A) Chemical structure of ailanthone. Seeding of (B) Cal-27 or (C) TCA8113 cells was done onto a 96-well plate followed by treatment with different concentrations (0.25, 0.5, 1, 2, 4, 8, 16, and 32 μM) of AIL for 24 h. *** $p < 0.001$,

compared with the control. Influence of AIL on apoptosis among (D) Cal-27 or (E) TCA8113 cells, as detected by Hoechst 33258 staining. The apoptotic rate of (F) Cal-27 or (G) TCA8113 cells after AIL treatment for 24 h was detected by employing Annexin V-FITC/PI double staining. The percent count of apoptotic cells in Cal-27 or TCA8113 cells is shown in (H) and (I). ** p < 0.01, *** p < 0.001, in comparison with the control cells.

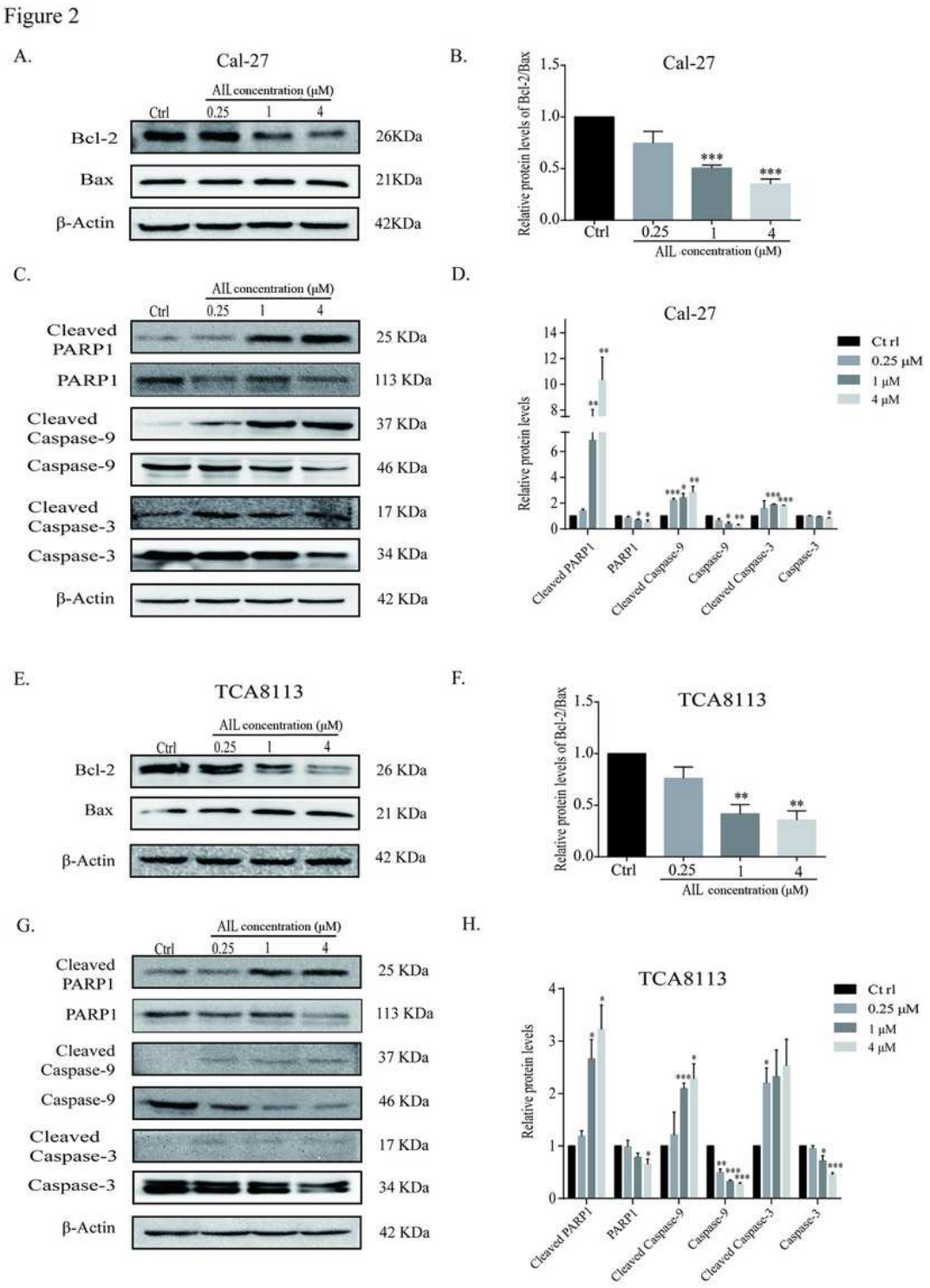

Figure 2

AIL induced apoptosis in TSCC by influencing Bcl-2/Bax ratio and caspase expression. (A) The protein expression of Bax and Bcl-2 in Cal-27 cells subjected to AIL treatment or otherwise were assessed by western blotting. (B) Statistical study of the Bcl-2/Bax ratio in Cal-27 cells with or without AIL. *** $p < 0.001$, compared with the control. (C) The degree of expression of cleaved PARP1, PARP1, cleaved caspase-9, caspase-9, cleaved caspase-3, and caspase-3 in Cal-27 cells was assessed by western blotting. (D) Statistical analysis of the expression of cleaved PARP1, PARP1, cleaved caspase-9, caspase-9, cleaved caspase-3, and caspase-3 in AIL-treated Cal-27 cells. * $p < 0.05$, ** $p < 0.01$, *** $p < 0.001$, in comparison with the control. (E) The protein expression of Bcl-2 and Bax in TCA8113 cells treated with or without AIL were examined by western blotting. (F) Statistical analysis of the Bcl-2/Bax ratio in TCA8113 cells with or without AIL. ** $p < 0.01$, compared with the control. (F) The extent of expression of cleaved PARP1, PARP1, cleaved caspase-9, caspase-9, cleaved caspase-3, and caspase-3 in TCA8113 cells were assessed by western blotting. (G) Statistical study of the expression of cleaved PARP1, PARP1, cleaved caspase-9, caspase-9, cleaved caspase-3, and caspase-3 in AIL-treated TCA8113 cells. * $p < 0.05$, ** $p < 0.01$, *** $p < 0.001$, in comparison with the control.

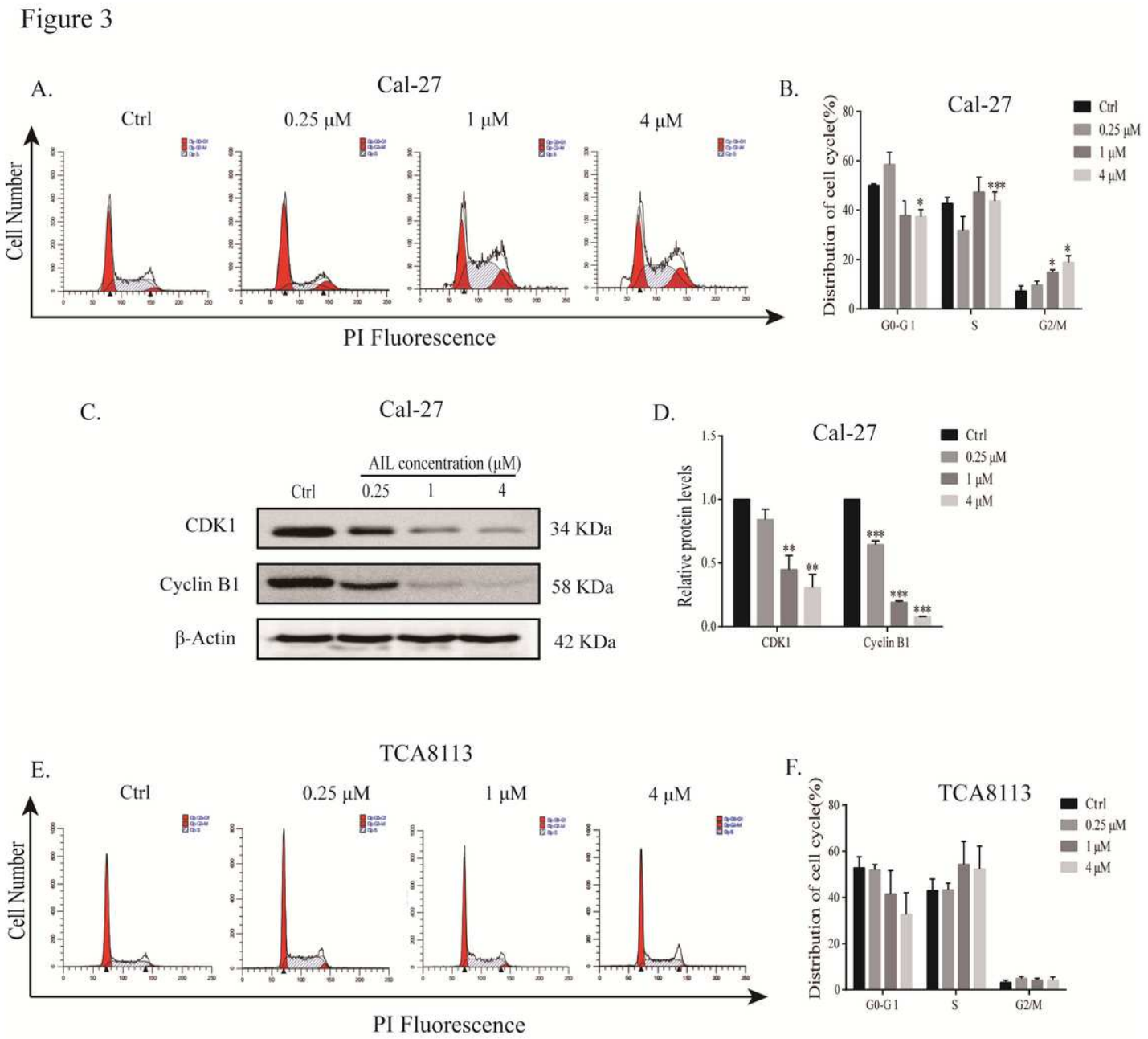

Figure 3

AIL induced cycle arrest in G2/M phase in Cal-27 cells, however did not have any influence on TCA8113 cells. (A) Flow cytometry was employed to analyze the cell cycle distribution changes in Cal-27 cells subjected to AIL treatment or otherwise. (B) Statistical analysis of the distribution of cell cycle in Cal-27 cells treated with or without AIL. * $p < 0.05$, *** $p < 0.001$, compared with the control. (C) The expression levels of CDK1 and Cyclin B1 in Cal-27 cells treated with or without AIL, as assessed by western blotting. (D) Statistical study of the expression levels of CDK1 and Cyclin B1 in AIL-treated Cal-27 cells. ** $p < 0.01$, *** $p < 0.001$, in comparison with the control. (E) The changes in cell cycle distribution in TCA8113 cells subjected to AIL treatment or otherwise were measured by flow cytometry. (F) Statistical study of the cell cycle distribution in TCA8113 cells treated with or without AIL. However, no significant changes were apparent in the AIL-treated TCA8113 cells in comparison with the controls.

Figure 4

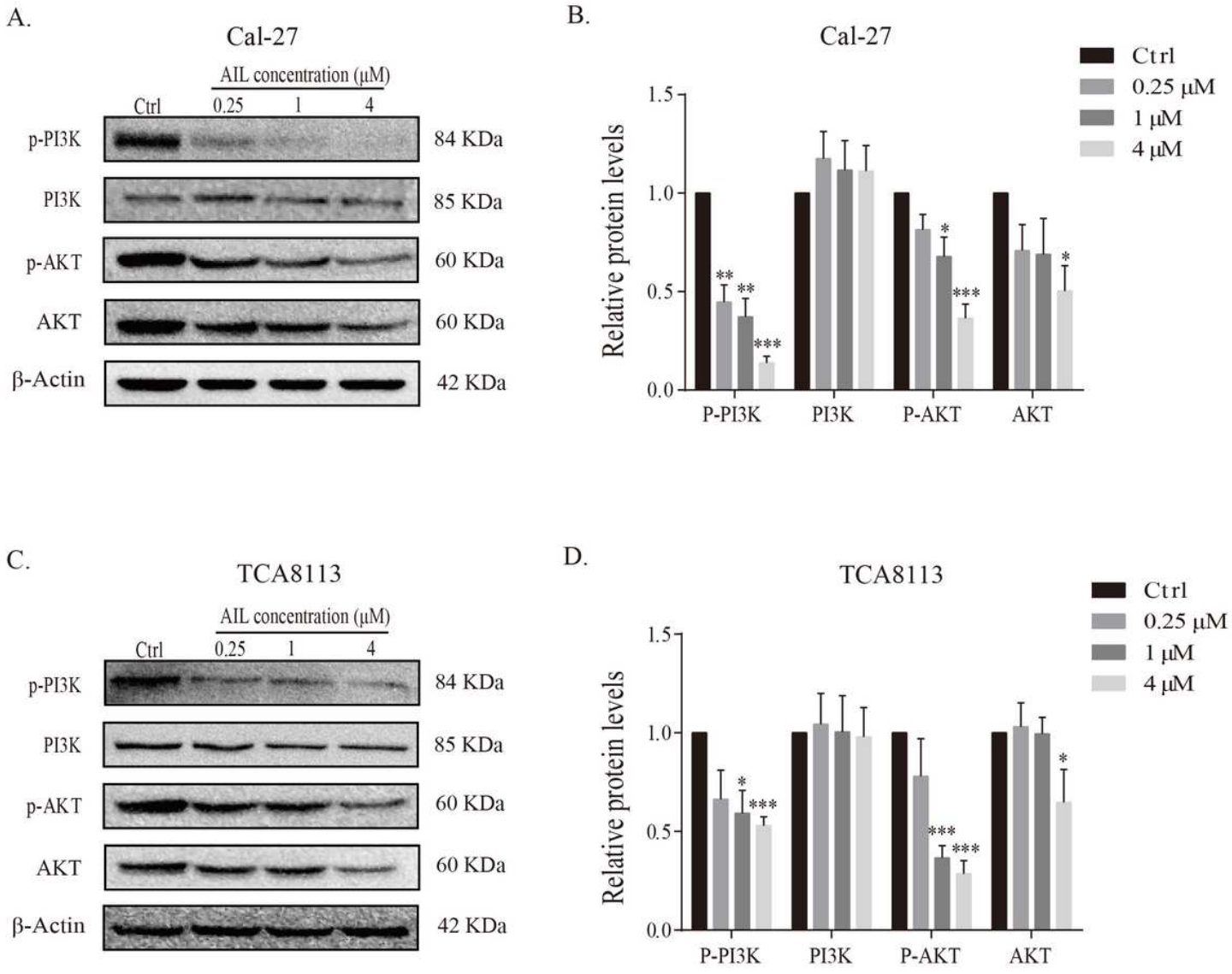

Figure 4

AIL decreased the proliferation of TSCC cells via the PI3K/AKT Pathway. (A) The extent of expression of p-PI3K, PI3K, p-AKT, and AKT in Cal-27 cells treated with or without AIL were ascertained by western blotting. (B) Statistical study of the expression levels of p-PI3K, PI3K, p-AKT, and AKT in the AIL-treated Cal-27 cells. * $p < 0.05$, ** $p < 0.01$, *** $p < 0.001$, in comparison with the control. (C) The expression levels of p-PI3K, PI3K, p-AKT, and AKT in TCA8113 cells treated with or without AIL were assessed by western blotting. (D) Statistical study of the expression levels of p-PI3K, PI3K, p-AKT, and AKT in the AIL-treated TCA8113 cells. * $p < 0.05$, ** $p < 0.01$, *** $p < 0.001$, in comparison with the control.